

# The Three-Dimensional Structure of an Arachidonic Acid 15-Lipoxygenase

Jeffrey C. Boyington, Betty J. Gaffney, L. Mario Amzel\*

In mammals, the hydroperoxidation of arachidonic acid by lipoxygenases leads to the formation of leukotrienes and lipoxins, compounds that mediate inflammatory responses. Lipoxygenases are dioxygenases that contain a nonheme iron and are present in many animal cells. Soybean lipoxygenase-1 is a single-chain, 839-residue protein closely related to mammalian lipoxygenases. The structure of soybean lipoxygenase-1 solved to 2.6 angstrom resolution shows that the enzyme has two domains: a 146-residue  $\beta$  barrel and a 693-residue helical bundle. The iron atom is in the center of the larger domain and is coordinated by three histidines and the  $\text{COO}^-$  of the carboxyl terminus. The coordination geometry is nonregular and appears to be a distorted octahedron in which two adjacent positions are not occupied by ligands. Two cavities, in the shapes of a bent cylinder and a frustum, connect the unoccupied positions to the surface of the enzyme. The iron, with two adjacent and unoccupied positions, is poised to interact with the 1,4-diene system of the substrate and with molecular oxygen during catalysis.

Arachidonic acid is the key precursor of a large family of potent physiological effectors. It is the branch point leading to two important pathways: one involves the enzyme cyclooxygenase and leads to the synthesis of prostaglandins and thromboxanes, whereas the other involves the lipoxygenase enzymes and leads to the synthesis of leukotrienes and lipoxins, compounds that regulate cellular response in inflammation and immunity (1, 2). Aspirin and related compounds are potent inhibitors of cyclooxygenases, but no comparable therapeutic inhibitors exist for the other pathway (1). This has led many laboratories to pursue the development of lipoxygenase inhibitors for use as anti-inflammatory agents in aspirin-insensitive inflammations.

Lipoxygenases are enzymes containing nonheme iron that use molecular oxygen in the dioxygenation of arachidonic acid to form hydroperoxides. Studies of lipoxygenases have included detailed kinetic measurements, cloning, expression, and site-directed mutagenesis. Nevertheless, answers to most of the fundamental structural and mechanistic questions about these enzymes have remained elusive, in part because of the lack of an atomic resolution model. We now describe the three-dimensional structure of soybean lipoxygenase-1 (839 residues, 94,262 daltons), a homolog of mammalian lipoxygenases (3, 4).

Lipoxygenases from both plant and ani-

mal tissues have been purified and characterized. In plants, the enzyme may participate in development, senescence, and in the production of antibacterial compounds (5). Sequences of 14 lipoxygenases have been reported, and several have been cloned and expressed as active proteins (6–8). They form a closely related family with no similarities to other known sequences. Crystals have been reported for several of these enzymes (9). The iron atom, which is essential for enzymatic activity, exists in two oxidation states:  $\text{Fe}^{2+}$  and  $\text{Fe}^{3+}$ ; in both forms the iron is high spin (spin 4/2 and spin 5/2, respectively) (10). Spectroscopic data show that the metal is bound to nitrogen- and oxygen-containing groups in the protein; it appears that heme or sulfur ligands are not present (11–13). The sequences of lipoxygenases share a highly conserved region of 38 amino acids, with 5 being histidine residues (7). In

addition, another conserved histidine occurs at a distance of 149 to 170 residues from the last amino acid in this group. These six histidines have been suggested as possible iron ligands.

**Structure determination.** Lipoxygenase-1, purified by a modification (13) of the method of Axelrod (14), was crystallized after more than a thousand crystallization conditions were tested (15). The crystals have the symmetry of space group  $C2$  and cell dimensions  $a = 184.5 \text{ \AA}$ ,  $b = 125.6 \text{ \AA}$ ,  $c = 94.7 \text{ \AA}$ , and  $\beta = 102.9^\circ$  and contain two molecules in the asymmetric unit (16); the solvent content is 56 percent. Dissolved crystals of enzyme had normal catalytic activity, an indication that the iron was retained during crystallization. The lack of color and the absence of an electron paramagnetic resonance (EPR) signal suggest that the iron is in the ferrous state in the crystal.

We calculated initial phases using three heavy atom derivatives: potassium dicyanoaurate(I), mersalyl, and mercuric cyanide (Table 1). The local symmetry element—a  $141.8^\circ$  rotation followed by a  $22.5 \text{ \AA}$  translation—was used in phase improvement cycles of density averaging and solvent flattening. The final average figure of merit was 0.82.

A sequence in the COOH-terminal portion was identified and used to start model building in both directions from this region with the program CHAIN (17). Connecting loops were in some cases difficult to build, but getting back in phase with the sequence of a helix or a sheet after building a connecting loop presented no problems. The complete polypeptide chain was traced unambiguously with the exception of three short loops on the surface of the protein (residues 67 to 74, 115 to 121, and 365 to 375) and the first five residues of the  $\text{NH}_2$ -terminus, which all are in regions of the map with poor or no electron density. The initial model was refined by conjugate gradient minimization with XPLOR (18) to an

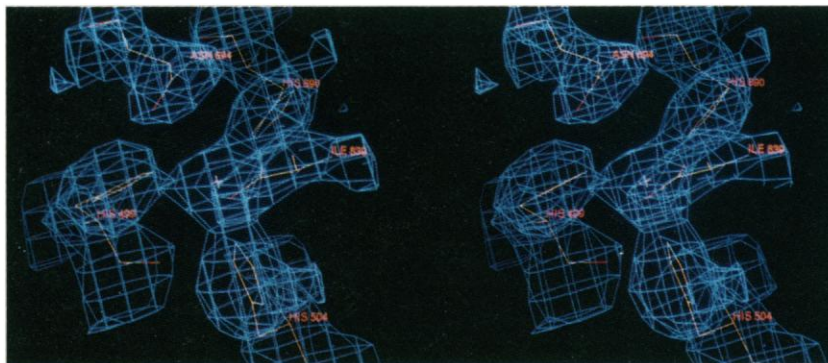


Fig. 1. Stereo view of a section of the final  $2F_o - F_c$  electron density map at the iron center of soybean lipoxygenase-1. The final model (in yellow) is superimposed on the electron density.

J. C. Boyington and L. M. Amzel are in the Department of Biophysics and Biophysical Chemistry, Johns Hopkins University School of Medicine, Baltimore, MD 21205. B. J. Gaffney is in the Department of Chemistry, Johns Hopkins University, Baltimore, MD 21218.

\*To whom correspondence should be addressed.

R value of 21.4 percent for the 46,136 reflections with  $F \geq 5\sigma$  between and 6.0 and 2.8 Å resolution ( $R = 22.0$  percent for the 51,290 reflections with  $F \geq 0.0\sigma$ ) while maintaining excellent geometry. The final  $2F_o - F_c$  map is of consistently high quality (Fig. 1) as are the omit maps,  $2F_o - F_c$  maps computed with structure factors calculated without including the portion of the molecule that was being plotted.

**Overall structure.** Lipoxigenase-1 is a two-domain, single-chain prolate ellipsoid of dimension 90 by 65 by 60 Å (Fig. 2). Domain I is an eight-stranded antiparallel  $\beta$  barrel with jelly roll-like topology that comprises the 146 NH<sub>2</sub>-terminal residues (Figs. 2 and 3). The interior of the barrel is

densely packed with hydrophobic side chains; many of them are aromatic. This domain is identical in connectivity to a similar  $\beta$  barrel observed in the COOH-terminal portion of human pancreatic lipase (involved in colipase binding) even though the two regions have no significant sequence similarity (19). Domain I makes only a loose contact with the rest of the molecule.

The major domain of the protein, domain II, comprises the COOH-terminal 693 residues in a bundle of 23 helices. Two antiparallel  $\beta$  sheets lie flat on the surface on opposite sides of the domain (Fig. 2). Seventeen of the 23 helices are approximately parallel or antiparallel to each other

and surround a long central helix of 43 residues that extends along the longest dimension of the molecule (Figs. 2 and 3). Although the central helix is surrounded on all sides by other helices, regions on each end are exposed to the solvent. The middle portion of this helix, although buried, is not predominantly hydrophobic. None of the helices is completely hydrophobic, but there is an extensive network of hydrophobic clusters in the domain, including five tryptophans that touch each other on one side of helix 17.

Domain II contains two distinct  $\pi$  helices (a  $\pi$  helix, with hydrogen bonding between residues  $i$  and  $i + 5$  instead of  $i$  and  $i + 4$ , is rare.) The  $\pi$  helices lie in the middle of the two largest helices in the molecule, and both contain residues serving as ligands to the iron. The first  $\pi$  helix, in helix 9, is the longest one reported so far for a globular protein. It consists of 13 residues (20) from His<sup>494</sup> to Ala<sup>506</sup>. Two of these residues, His<sup>499</sup> and His<sup>504</sup>, are iron ligands. The second  $\pi$  helix (six residues, Ile<sup>685</sup> to His<sup>690</sup>) occurs in helix 18 and contains His<sup>690</sup>, the third iron ligand. The three-dimensional structure of lipoxigenase-1 has 38 percent  $\alpha$  helix and 14 percent  $\beta$  sheet.

**Coordination of the iron.** The iron in lipoxigenase-1 is coordinated to four ligands at the center of domain II. The coordination can be best described as a highly distorted octahedron with two adjacent, unoccupied positions (Figs. 1 and 4 and Table 2). (An alternative description is a tetrahedron in which one ligand position is significantly distorted from tetrahedral geometry.) Three of the coordination positions are occupied by the Ne of the three histidine residues described above (His<sup>499</sup>, His<sup>504</sup>, and His<sup>690</sup>), and the fourth position is occupied by an oxygen of the COOH-terminus (residue Ile<sup>839</sup>). The carboxylate provides the only negative charge in the immediate vicinity of the iron. The oxygen is about 1.5 Å away from the position expected for a tetrahedral arrangement, resulting in an O-Fe-N angle with the Ne of His<sup>499</sup> of 150.8° (164.6° in molecule 2), close to the 180° angle expected for octahedral coordination (Table 2). The three Fe-N and the Fe-O distances (Table 2) are similar to other distances observed in small molecule iron complexes (21). The plane defined by the Ne atoms of the three imidazole ligands can be considered the base of the distorted tetrahedron. The planes of all three imidazole rings are perpendicular to this base. All the C $\delta$ -Ne-Fe and C $\epsilon$ -Ne-Fe angles formed by the ligands are close to 120°. Two of the Fe-Ne bonds are in the plane of their imidazole rings. The third Fe-Ne bond (His<sup>499</sup>), in contrast, makes a 33.0° angle with the plane of the imidazole ring, suggesting the possibility of  $sp^3$  hybrid-

**Table 1.** Structure determination. Intensity data were collected at room temperature with a Siemens area detector equipped with a Rigaku RU200 rotating anode generator and a graphite monochromator. Data were processed with the package XENGEN (28). Scaling, phasing, and heavy atom parameter refinement were done with programs in the package PROTSYS (29). Multiple isomorphous replacement phases were improved by successive rounds of solvent flattening (30) and refinement of heavy atom parameters against the improved phases. On the basis of the heavy atom positions, the noncrystallographic symmetry relating the two molecules of the asymmetric unit was uniquely determined. Phases were further improved by iterative cycles of density averaging and phase combination with a heavily modified version of an averaging program (31). Anomalous scattering data from both derivatives were also used. During the phase improvement process, a large number of maps were calculated on the basis of combinations of heavy atom phases, solvent flattening, and symmetry averaging. Many of these maps showed outstanding resolution and definition in certain regions of the cell. These maps were used as an aid for building in regions where the final map showed poor density. The model was built manually with the program CHAIN (17), and its positional and thermal parameters were refined by conjugate gradients with XPLOR (18). Low weight constraints were introduced to maintain approximate noncrystallographic symmetry, and values between 1.5 $\sigma$  and 2.5 $\sigma$  were used to constrain the temperature factors. During the last stages of the refinement, a resolution-dependent weighting scheme was applied to the individual reflections. Several water molecules were identified in relevant regions of the molecule but have not yet been included in the refinement.

Data collection						
Data set	Resolution (Å)	Measurements	Unique reflections (%)			$R_{\text{merge}} (\%)^*$
Native (2 crystals)	2.5	215,702	60,462 (82.5)			7.6
Hg(CN) <sub>2</sub>	2.8	81,790	38,514 (75.0)			5.8
Mersalyl†	2.8	72,494	44,139 (87.9)			7.6
KAu(CN) <sub>2</sub>	2.8	69,083	43,708 (87.0)			5.1
Phasing statistics‡						
Derivative	Soaking conditions		Sites	Average isomorphous difference (%)	$R_{\text{centric}}^{\S}$	Phasing power
	Conc. (mM)	Time (days)				
Hg(CN) <sub>2</sub>	1.0	71	6	16.7	0.46	2.26
Mersalyl†	0.8	2	4	13.5	0.54	1.72
KAu(CN) <sub>2</sub>	1.0	2	2	11.8	0.70	0.68
Refinement statistics						
Reflections (6.0 to 2.6 Å)	46,136 ( $F > 5\sigma_F$ )					
Nonhydrogen atoms	12,880					
R value	0.214			Solvent atoms	0	
rms deviation from ideality				Average B-factor	22.33 Å <sup>2</sup>	
Bond lengths	0.012 Å					
Bond angles	3.28°					
Improper torsion angles	1.36°					

\* $R_{\text{merge}} = \sum_i \sum_h |I_{ih} - \langle I_{ih} \rangle| / \sum_i \sum_h I_{ih}$ , where  $h$  are unique reflection indices and  $i$  indicates symmetry equivalent indices. †2-[N-[3-(hydroxymercuri-2-methoxypropyl)carbamoyl]phenoxy]acetic acid, sodium salt; C<sub>13</sub>H<sub>16</sub>HgNNaO<sub>6</sub>. ‡The combined figure of merit with the Hg(CN)<sub>2</sub> and mersalyl derivatives was 0.63. All data to 2.8 Å resolution with  $F > 3\sigma_F$  were used. § $R_{\text{centric}} = \sum_h (|F_{PH} - \bar{F}_P| - |f_H|) / \sum_h |F_{PH} - \bar{F}_P|$ . ||Phasing power =  $f_{\text{rms}} / E_{\text{rms}}$ , where  $f_{\text{rms}} = [(\sum_h f_H^2) / n]^{1/2}$  and  $E_{\text{rms}} = [(\sum_h (F_{PH} - \bar{F}_P)^2) / n]^{1/2}$ .

ization for this nitrogen (Figs. 1 and 4). Although it is possible to build the side chain at the position of His<sup>499</sup> in a conformation similar to that of the other two histidine ligands, electron-density maps calculated with this residue omitted indicate clearly that the imidazole ring occupies the position described above. The orientation of the three histidine ligands is determined by their locations in regions of  $\pi$  helices and by their participation in a network of hydrogen bonds mediated by both main chain and side chain atoms (Figs. 1 and 4). The N $\delta$  of His<sup>499</sup> is hydrogen-bonded to the side chain of Gln<sup>495</sup> at the beginning of a series of hydrogen bonds that connect Gln<sup>697</sup>, Asn<sup>694</sup>, and the main chain carbonyl of Leu<sup>754</sup>. The N $\delta$  of His<sup>504</sup> is hydrogen-bonded to the side chain of Asn<sup>539</sup>. Similarly, His<sup>690</sup> appears to be hydrogen-bonded through a water to the main chain carbonyls of Ser<sup>836</sup> and Ser<sup>687</sup>. The N $\delta$  of Asn<sup>694</sup>, which is part of this network, is only 3.3 Å from the iron and very close to the unoccupied coordination position opposite to His<sup>504</sup>. In all lipoxygenases, the Asn<sup>694</sup> is highly conserved and it is replaced by histidine in only four of the sequences.

The coordination of the iron with only four ligands in a distorted octahedral arrangement leaves two unoccupied ligand positions. Because the spectroscopic evidence (22) suggests more than four iron ligands, the possible presence of fifth and sixth ligands (such as a water molecule or a hydroxyl group) was investigated in detail. Difference ( $F_o - F_c$ ) maps and  $2F_o - F_c$  maps calculated with data from 50 to 2.6 Å in the region close to the iron showed no significant density in the position expected for these ligands (Fig. 1). It is possible, however, that these positions become occupied during the catalytic cycle of the enzyme. Given the information presented in this article it would be useful to reevaluate the EXAFS, Mössbauer, and other spectroscopic data.

Tetrahedral iron is not common in small molecule complexes of either Fe<sup>2+</sup> or Fe<sup>3+</sup>, which appear to favor the formation of six-coordinate octahedral complexes. However, ligand coordination similar to that of lipoxygenase has been observed in iron superoxide dismutase (23). In both proteins, the iron is coordinated by three histidines and one carboxylate, the terminal carboxylate in lipoxygenase and a glutamate in superoxide dismutase. Both proteins have similar Fe-O and Fe-N distances, but the coordination is distorted from the tetrahedron in a different manner in the two structures, being closer to a trigonal bipyramid in superoxide dismutase. The similarity of the iron centers is not a consequence of an overall similarity between the two proteins because they have no

sequence similarity and completely different folding patterns. Even the structural elements that provide the side chains for iron coordination differ in the two proteins.

**Internal cavities.** The coordinated iron

faces two large internal cavities that can connect the metal to the exterior of the molecule. Cavity I is conical and forms a tunnel that connects the position opposite to the Ne of His<sup>504</sup> to the surface of the

**Fig. 2.** Schematic diagram of the three-dimensional structure of soybean lipoxygenase-1. The  $\alpha$  helices are represented by cylinders, the strands in the  $\beta$  sheets by arrows, the coils by narrow rods, and the iron by a yellow ball. Only three of the four iron ligands are shown. Domain I, consisting of a single  $\beta$  barrel, is on the left. Domain II contains the iron, all the helices in the structure, and two small  $\beta$  sheet structures that lie on the surface of the enzyme.

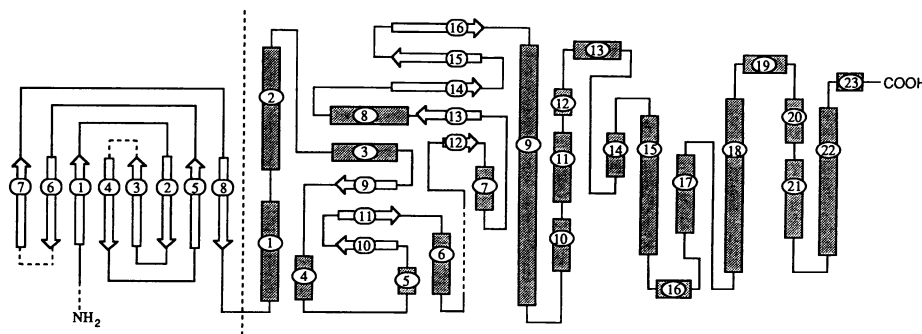
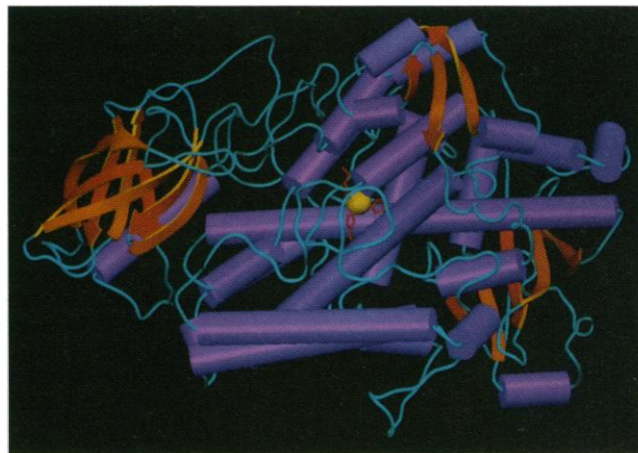


**Fig. 3.** Schematic diagram of the secondary structure of soybean lipoxygenase-1. The helices are represented by shaded rectangles, the  $\beta$  sheet strands by the arrows, and the connecting loops by continuous lines (20). Domain I is to the left of the vertical dotted line and domain II is to the right. The  $\beta$  strands (1 to 16) and the helices (1 to 23) are numbered in the order in which they appear in the structure. Helices represented as vertical rectangles are almost parallel (average angle 28°) to the major helix, number 9, and the horizontal ones are almost perpendicular (average angle 73°) to it. The lengths of the rectangles are approximately proportional to the length of the helices. Dotted lines represent regions that were not built into the model. In domain I the eight strands extend between the following residues: strand 1, 7 to 15; strand 2, 40 to 48; strand 3, 57 to 65; strand 4, 78 to 85; strand 5, 95 to 102; strand 6, 106 to 114; strand 7, 123 to 131; and strand 8, 141 to 145.

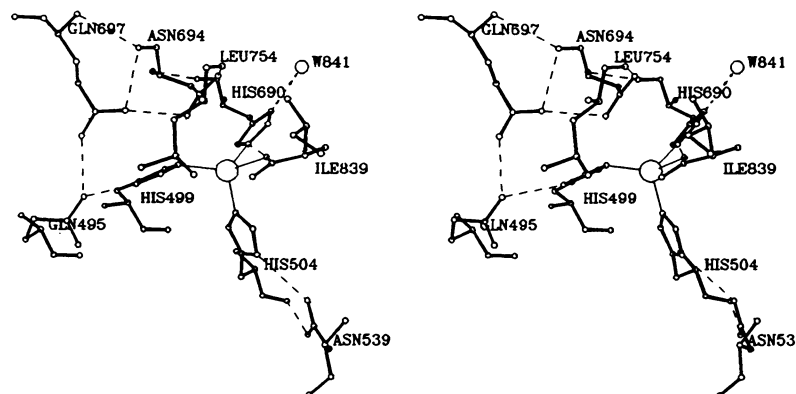


**Fig. 4.** Stereo view of the iron center in lipoxygenase-1. The residues His<sup>499</sup>, His<sup>504</sup>, His<sup>690</sup>, and the terminal carboxylate group of Ile<sup>839</sup> are directly coordinated to the iron. Dotted lines are hydrogen bonds.

protein (Fig. 5). The tunnel is 18 Å in length. It is 8 Å in diameter for most of its length but widens to 11 Å at the surface and narrows to 2.5 Å close to the iron center. The sides of the tunnel are lined by the side chains of 29 residues, most of which are hydrophobic (24). Some of these residues are conserved (or have only conservative substitutions) among all sequenced plant and mammalian lipoxygenases. This tunnel presents an ideal path for the movement of molecular oxygen from the outside into one of the two unoccupied coordination sites of the iron.

Cavity II faces the terminal COO<sup>-</sup> and two of the histidine ligands (His<sup>499</sup> and His<sup>504</sup>). This 40 Å long, narrow cavity (less than 3.5 Å in some places) changes direction by more than 90° at two places (Fig. 5). One bend is adjacent to the iron center,

close to the end of the cavity. Arachidonic acid (C<sub>20</sub>), or even a slightly larger fatty acid, can fit snugly into the end of this bent region, toward the innermost portion of the cavity. Arachidonic acid bound in this manner would approach the iron with the 11,14-diene system opposite His<sup>690</sup>. Sequence comparisons of the different lipoxygenases reveal a high degree of conservation for the 46 residues lining this cavity (25). Most of the residues are either hydrophobic or neutral with the exception of Glu<sup>349</sup>, Asp<sup>490</sup>, and three positively charged residues—His<sup>494</sup>, Arg<sup>707</sup>, and Lys<sup>483</sup>. The Lys<sup>483</sup> is near to the surface of the protein, but the other four residues are internal. Approximately in the middle, at the other bend, this cavity becomes narrow but can be widened by a small rearrangement of the side chains of Arg<sup>707</sup> and Val<sup>354</sup>.

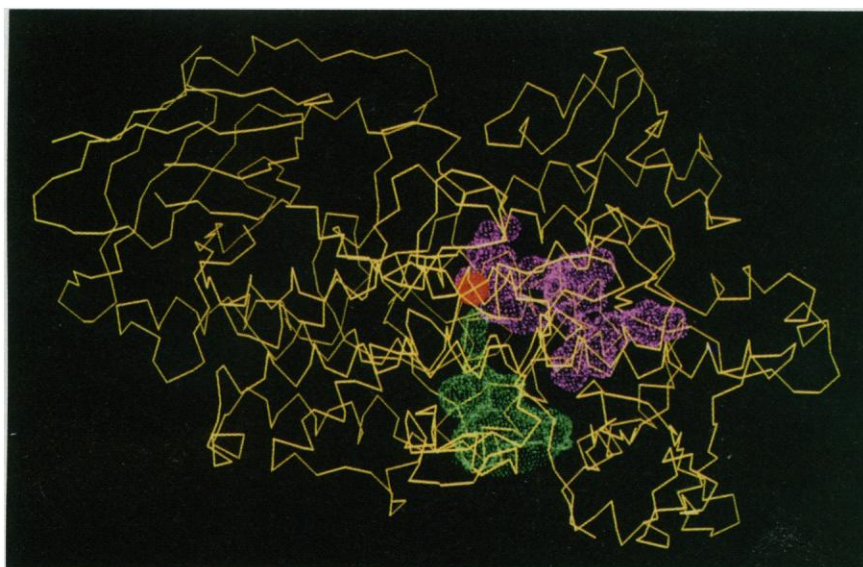


**Fig. 5.** Location of cavities I and II in lipoxygenase-1. The surfaces of the cavities, represented by dots (33), are superimposed on the  $\alpha$  carbon trace of the enzyme. Cavity I is in green, cavity II is in violet, and the iron is in orange.

**Table 2.** Coordination geometry at the iron center. The geometry for both molecules in the asymmetric unit (monomer 1 and monomer 2) is displayed. OT2, COO<sup>-</sup> terminal oxygen number 2.

Metal-ligand distances (Å)		
Bonds	Monomer 1	Monomer 2
Fe-His <sup>499</sup> N $\epsilon$	2.29	2.27
Fe-His <sup>504</sup> N $\epsilon$	2.13	2.24
Fe-His <sup>690</sup> N $\epsilon$	2.19	2.19
Fe-Ile <sup>839</sup> OT2	2.07	2.08
Ligand-metal-ligand angles (degrees)		
Angles	Monomer 1	Monomer 2
His <sup>499</sup> N $\epsilon$ -Fe-His <sup>504</sup> N $\epsilon$ *	102.6	102.2
His <sup>499</sup> N $\epsilon$ -Fe-His <sup>690</sup> N $\epsilon$ *	100.9	109.6
His <sup>504</sup> N $\epsilon$ -Fe-His <sup>690</sup> N $\epsilon$ *	104.0	101.4
His <sup>690</sup> N $\epsilon$ -Fe-Ile <sup>839</sup> OT2*	78.1	73.5
His <sup>504</sup> N $\epsilon$ -Fe-Ile <sup>839</sup> OT2*	106.0	91.7
His <sup>499</sup> N $\epsilon$ -Fe-Ile <sup>839</sup> OT2†	150.8	164.6

\*109.5° in a tetrahedron and 90.0° in an octahedron.

†109.5° in a tetrahedron and 180.0° in an octahedron.

The largest cavity is observed in the region between domains I and II. It is an oblate ellipsoid of dimension 11 by 18 by 19 Å and is connected to the surface by a short, narrow elliptical channel with a cross section of approximately 5 by 7 Å. This cavity, like the other two, is lined mostly by hydrophobic or neutral residues. It is neither close to nor connected with the other cavities or the iron site; it may be simply an interdomain space.

**Structure of other lipoxygenases.** The sequences of the three soybean lipoxygenases are similar; pairwise comparisons show identities of as great as 81 percent, with most substitutions being conservative. Analysis of the locations of the least conservative mutations and of the deletions and insertions in the structure of lipoxygenase-1 suggests that even these changes would be easy to accommodate without major changes in the structure.

The structure of soybean lipoxygenase-1 offers a natural explanation for the difference in length between the plant and mammalian enzymes. The plant enzymes contain both domains I and II, but in the mammalian enzymes only domain II is present. There are, in addition, five regions in domain II of the mammalian enzymes that have long deletions with respect to soybean lipoxygenase-1: the loop between helices 5 and 6, the loop between helices 14 and 15, the region corresponding to the COOH-terminal end of helix 19, the NH<sub>2</sub>-terminal end of helix 20 and the intervening loop, and the short helix 23 and the following loop. These regions all occur in solvent-exposed regions of the structure where they can be accommodated without major changes in the overall structure, suggesting that the structure of domain II of soybean lipoxygenase-1 can provide a good initial model for the interpretation of mutational and other data in the animal enzymes.

Single amino acid replacement at three of the six conserved histidines in soybean lipoxygenase-1 (His<sup>499</sup>, His<sup>504</sup>, and His<sup>690</sup>) (7) or in human 5-lipoxygenase (26) produces completely inactive enzymes. Replacement of any one of the other three histidines (His<sup>494</sup>, His<sup>522</sup>, and His<sup>531</sup>; His<sup>362</sup>, His<sup>390</sup>, and His<sup>399</sup> in human 5-lipoxygenase) produces enzymes with reduced but detectable enzymatic activity. The only other mutation that produces a completely inactive enzyme is the deletion of the six COOH-terminal amino acids of the soybean enzyme. As mentioned above, the terminal COO<sup>-</sup> provides the fourth iron ligand and the only negative charge in the vicinity of the iron. The terminal COO<sup>-</sup> reaches the iron as part of a long strand that extends from the surface of the molecule to the internal position occupied by the metal. If the strand were to be

shortened by six residues, it would be impossible for the terminal COO<sup>-</sup> to approach closely enough to the metal to act as a ligand. Thus, only mutations that change iron ligands produce completely inactive enzyme.

**Mechanism of lipoxygenases.** In the catalytic mechanisms proposed for lipoxygenase, the Fe<sup>3+</sup> form of the enzyme abstracts one electron from the fatty acid substrate, and a base on the enzyme accepts a proton from the 3 position of the substrate 1,4-pentadiene. The resulting intermediate could be described as having an Fe<sup>3+</sup>-carbon bond to substrate or an Fe<sup>2+</sup>-substrate free radical complex. Molecular oxygen reacts with the intermediate, regenerating Fe<sup>3+</sup> and producing a peroxidate anion. The peroxidate then receives the proton from the base on the enzyme to give the hydroperoxide product (4, 27).

The structure of lipoxygenase-1 suggests how some of these events might occur in the peroxidation of, for example, arachidonic acid. The fatty acid enters cavity II after small movements of the side chains of Leu<sup>480</sup> and Met<sup>341</sup>. In the cavity, arachidonic acid approaches the iron such that the 11,14-diene system moves into the unoccupied octahedral position opposite His<sup>690</sup>. Possible candidates for the base that accepts the proton are the Ne of His<sup>499</sup> and the second oxygen of the terminal COO<sup>-</sup> (Ile<sup>839</sup>). Abstraction of the *pro-S* (L<sub>S</sub>) proton from C-13 and interaction of Fe<sup>3+</sup> with C-15 to form an Fe-C bond or Fe<sup>2+</sup> and a free radical can occur in this arrangement. Molecular oxygen enters the molecule through the tunnel and coordinates with iron in the unoccupied position opposite the Ne of His<sup>504</sup>. (The side chain of Asn<sup>694</sup> can reorient and form a hydrogen bond with the bound oxygen.) In this situation, molecular oxygen is in a location well suited for reacting with C-15 of the arachidonic acid to produce a peroxidate anion and Fe<sup>3+</sup>. The peroxidate anion is protonated and released, and the coordination of the iron returns to that at the beginning of the catalytic cycle. This sequence of events is compatible with most experimental evidence and incorporates the salient features of the three-dimensional structure.

## REFERENCES AND NOTES

1. B. Samuelsson, *Science* **220**, 568 (1983).
2. S.-E. Dahlén, J. Å. Lindgren, C. A. Rouzer, C. N. Serhan, *ibid.* **237**, 1171 (1987).
3. According to the nomenclature of H. Kühn, T. Schewe, and S. M. Rapoport [*Adv. Enzymol. Relat. Areas Mol. Biol.* **58**, 273 (1986)], soybean lipoxygenase-1 is a [C<sub>n</sub>-S]<sup>-L<sub>pro-S</sub></sup>[+2]-L<sub>S</sub> lipoxygenase; it oxidizes arachidonic acid at C-15 and linoleic acid at C-13. The prochiral *pro-S* proton and the *S* hydroperoxide were found to be the L stereoisomers.
4. T. Schewe, S. M. Rapoport, H. Kühn, *ibid.*, p. 191.
5. H. W. Gardner, *Biochim. Biophys. Acta* **1084**, 211 (1991); K. P. C. Croft, F. Jüttner, A. J. Slusarenko, *Plant Physiol.* **101**, 13 (1993).
6. J. Steczko, G. A. Donoho, J. E. Dixon, T. Sugimoto, B. Axelrod, *Protein Expr. Purif.* **2**, 221 (1991).
7. J. Steczko, G. P. Donoho, J. C. Clemens, J. E. Dixon, B. Axelrod, *Biochemistry* **31**, 4053 (1992).
8. N. DeMarzo, D. L. Sloane, S. Dicharry, E. Highland, E. Sigal, *Am. J. Physiol.* **262**, L198 (1992); C. D. Funk, L. Furci, G. A. FitzGerald, *Proc. Natl. Acad. Sci. U.S.A.* **87**, 5638 (1990); J. M. Balcarek *et al.*, *J. Biol. Chem.* **263**, 13937 (1988); T. Matsumoto *et al.*, *Proc. Natl. Acad. Sci. U.S.A.* **85**, 26 (1988); D. Shibata *et al.*, *J. Biol. Chem.* **262**, 10080 (1987); D. Shibata *et al.*, *ibid.* **263**, 6816 (1988); E. Sigal *et al.*, *Biochem. Biophys. Res. Commun.* **157**, 457 (1988); T. Yoshimoto *et al.*, *Proc. Natl. Acad. Sci. U.S.A.* **87**, 2142 (1990); R. A. F. Dixon *et al.*, *ibid.* **85**, 416 (1988); P. M. Ealing and R. Casey, *Biochem. J.* **253**, 915 (1988); *ibid.* **264**, 929 (1989); J. Fleming *et al.*, *Gene* **79**, 181 (1989); D. Shibata, T. Kato, K. Tanaka, *Plant Mol. Biol.* **16**, 353 (1991); H. Ohta, Y. Shirano, K. Tanaka, Y. Morita, D. Shibata, *Eur. J. Biochem.* **206**, 331 (1992).
9. J. Steczko, C. R. Muchmore, J. L. Smith, B. Axelrod, *J. Biol. Chem.* **265**, 11362 (1990); W. C. Stallings, B. A. Kroa, R. T. Carroll, A. L. Metzger, M. O. Funk, *J. Mol. Biol.* **211**, 685 (1990); D. L. Sloane, M. F. Browner, Z. Dauter, K. Wilson, R. J. Fletterick, E. Sigal, *Biochem. Biophys. Res. Commun.* **173**, 507 (1990).
10. T. M. Cheesbrough and B. Axelrod, *Biochemistry* **22**, 3837 (1983).
11. W. R. Dunham, R. T. Carroll, J. E. Thompson, R. H. Sands, M. O. Funk, Jr., *Eur. J. Biochem.* **190**, 611 (1990).
12. S. Navratnam *et al.*, *Biochim. Biophys. Acta* **956**, 70 (1988).
13. B. J. Gaffney, D. V. Mavrophilipos, K. S. Doctor, *Biophys. J.* **64**, 773 (1993).
14. B. Axelrod, T. M. Cheesbrough, S. Laasko, *Methods Enzymol.* **71**, 441 (1981).
15. Lipoxygenase was crystallized by hanging drop vapor diffusion in 4.6 M sodium formate, 1.0 M ammonium acetate, 600 mM lithium chloride, 20 mM 2-(*N*-morpholino)ethanesulfonic acid, and protein at 15 to 20 mg/ml (pH 7.0). Conditions slightly different from the optimal or missing any of the components produced only precipitate or needle-shaped crystals not suitable for diffraction studies.
16. J. C. Boyington, B. J. Gaffney, L. M. Amzel, *J. Biol. Chem.* **265**, 12771 (1990).
17. J. S. Sack, *J. Mol. Graphics* **6**, 244 (1988).
18. A. T. Brünger, J. Kuriyan, M. Karplus, *Science* **235**, 458 (1987).
19. F. K. Winkler, A. D'Arcy, W. Hunziker, *Nature* **343**, 771 (1990).
20. The secondary structure elements were identified with the algorithm of W. Kabsch and C. Sander [*Biopolymers* **22**, 2577 (1983)].
21. D. C. Finneh, A. A. Pinkerton, W. R. Dunham, R. H. Sands, M. O. Funk, Jr., *Inorg. Chem.* **30**, 3960 (1991).
22. Spectroscopic studies to determine the coordination of the iron in ferrous lipoxygenases have favored octahedral coordination of the metal. On the basis of magnetic circular dichroism data, the effective site symmetry of ferrous soybean lipoxygenase-1 was assigned as distorted octahedral [J. W. Whittaker and E. I. Solomon, *J. Am. Chem. Soc.* **110**, 5329 (1988)]. EXAFS studies were best interpreted as indicating the presence of 6 ± 1 nitrogen or oxygen atoms (in any combination) at distances of 2.05 to 2.09 Å from the iron [L. M. Van der Heijden *et al.*, *Eur. J. Biochem.* **207**, 793 (1992)]. The quadrupole splitting parameter from Mossbauer measurements is also consistent with distorted octahedral ligand symmetry (17).
23. B. L. Stoddard, P. L. Howell, D. Ringe, G. A. Petsko, *Biochemistry* **29**, 8885 (1990).
24. These residues are: Cys<sup>357</sup>, Val<sup>358</sup>, Ile<sup>359</sup>, Arg<sup>360</sup>, Tyr<sup>409</sup>, Ile<sup>412</sup>, Tyr<sup>493</sup>, Met<sup>497</sup>, Ser<sup>498</sup>, His<sup>499</sup>, Leu<sup>501</sup>, Asn<sup>502</sup>, Thr<sup>503</sup>, Val<sup>570</sup>, Asn<sup>573</sup>, Trp<sup>574</sup>, Val<sup>575</sup>, Asp<sup>578</sup>, Gln<sup>579</sup>, Leu<sup>581</sup>, Asp<sup>584</sup>, Lys<sup>587</sup>, Arg<sup>588</sup>, Tyr<sup>610</sup>, Trp<sup>684</sup>, Leu<sup>688</sup>, His<sup>690</sup>, and Val<sup>693</sup>.
25. The following residues are completely conserved across all 14 known lipoxygenase sequences: Trp<sup>340</sup>, Phe<sup>346</sup>, Gly<sup>353</sup>, Asn<sup>355</sup>, Lys<sup>483</sup>, Asp<sup>490</sup>, His<sup>494</sup>, His<sup>499</sup>, His<sup>504</sup>, Ala<sup>542</sup>, Leu<sup>546</sup>, Glu<sup>697</sup>, Asn<sup>706</sup>, and Leu<sup>754</sup>. One residue of this cavity, Phe<sup>557</sup> (Met<sup>418</sup> in the human 15-lipoxygenase), was shown by site directed mutagenesis to be involved in determining the positional specificity of the enzyme [D. L. Sloane, R. Leung, C. S. Craik, E. Sigal, *Nature* **354**, 149 (1991)].
26. T. Nguyen, J.-P. Falguyret, M. Abramovitz, D. Riendeau, *J. Biol. Chem.* **266**, 22057 (1991); Y. Y. Zhang, O. Rådmark, B. Samuelsson, *Proc. Natl. Acad. Sci. U.S.A.* **89**, 485 (1992).
27. Evidence in favor of an Fe<sup>3+</sup>-carbon intermediate has been provided by kinetic studies with variations in substrate structure and by chemical analogy [E. J. Corey and R. Nagata, *J. Am. Chem. Soc.* **109**, 8701 (1987); E. J. Corey and J. C. Walker, *ibid.*, p. 8108]. Evidence for the Fe<sup>2+</sup>-free radical pathway is based on anaerobic reduction of Fe<sup>3+</sup> by fatty acid substrate (10) and on detection of substrate free radicals [J. J. M. de Groot, G. J. Garssen, J. F. G. Vligenthart, J. Boldingh, *Biochim. Biophys. Acta* **326**, 279 (1973); W. Chamulitrat and R. P. Mason, *J. Biol. Chem.* **264**, 20968 (1989); M. J. Nelson, S. P. Seitz, R. A. Cowling, *Biochemistry* **29**, 6897 (1990)]. An Fe<sup>3+</sup>-carbon bond could undergo anaerobic dissociation to form Fe<sup>2+</sup> and a free radical (Corey and Nagata). Thus the nature of the interaction of oxygen with the enzyme-substrate complex is the key point that distinguishes the different mechanistic proposals.
28. A. J. Howard *et al.*, *J. Appl. Crystallogr.* **20**, 383 (1987).
29. PROTSYS was implemented by G. Petsko.
30. B. C. Wang, *Methods Enzymol.* **115**, 90 (1985).
31. The program was written by J. Smith and W. Hendrickson.
32. The drawing was made with the program SETOR, courtesy of S. Evans.
33. Generated by the program MS [M. L. Connolly, *J. Appl. Crystallogr.* **16**, 548 (1983)] with a probe radius of 1.2 Å [A. A. Rashin, I. Michael, B. Honig, *Biochemistry* **25**, 3619 (1986)]. The volume of cavity II is 819 Å<sup>3</sup> for the 1.2 Å probe radius and 653 Å<sup>3</sup> if the 1.4 Å probe radius is chosen.
34. We thank E. Lattman, J. Berg, and J. Wehrle for reviewing the manuscript and for suggestions. The coordinates have been deposited in the Brookhaven Protein Data Bank. Computing and x-ray diffraction facilities were purchased with grants from NSF, NIH, and the Keck Foundation and supported by NSF, the Keck Foundation, and the Lucille P. Markey Charitable Trust. B.J.G. was supported by National Institutes of Health grant GM36232.

8 February 1993; accepted 14 May 1993